Caballero-Mancebo, E.; Moreno-Rodríguez, JM.; Cohen, B.; Díaz Morales, UM.; Corma Canós, A.; Douhal, A. (2018). Unraveling Competitive Electron and Energy-Transfer Events at the Interfaces of a 2D MOF and Nile Red Composites: Effect of the Length and Structure of the Linker. ACS Applied Materials & Interfaces. 10(38):32885-32894. https://doi.org/10.1021/acsami.8b12188

Unravelling Competitive Electron and Energy Transfer Events at the Interfaces of a 2D-MOF and Nile Red Composites: Effect of the Length and Structure of the Linker

Elena Caballero-Mancebo[a], José María Moreno[b], Boiko Cohen[a], Urbano Díaz[b], Avelino Corma[b] and Abderrazzak Douhal[a*]

[a]Departamento de Química Física, Facultad de Ciencias Ambientales y Bioquímica, and INAMOL, Universidad de Castilla-La Mancha, Avenida Carlos III, S/N, 45071 Toledo, Spain.

[b]Instituto de Tecnología Química, Universitat Politecnica de Valéncia-Consejo Superior de Investigaciones Científicas (UPV-CSIC), Av. de los Naranjos s/n, 46022 Valencia, Spain.

*corresponding author: Abderrazzak.Douhal@uclm.es

KEYWORDS: hybrid materials, interfaces, composite, energy transfer, electron transfer.

ABSTRACT

The distribution and interactions of organic molecules adsorbed on the surface of materials play important roles in many catalytic and photonic processes. Here, we show that the length and chemical structure of the linker in new Al-ITQ MOFs are fundamental for the dynamics of the dye Nile Red adsorbed on its surface. For the studied composites using Al-ITQ-EB, Al-ITQ-AB and Al-ITQ-EB exposed to the aniline (AN) or N, N-dimethylaniline (DMA) atmospheres, we observed a very fast (~ 1.2 ps) intramolecular charge transfer (ICT) reaction in adsorbed NR molecules. For NR@Al-ITQ-EB, where the linker has a shorter aliphatic chain (2 carbons), the dye molecules present a homo energy transfer (ET) process, which is faster (~90 ps) than in the previously reported NR@Al-ITQ-HB composite with longer aliphatic chain (7 carbons, ~220 ps). The more polar environment created by the Al-oxide nodes in Al-ITQ-EB surface around the NR populations strongly favours the ET event. When the linker structure contains phenyl amine moieties, the resulting NR@Al-ITQ-AB composites, shows different and rich photodynamics, in which a fast electron transfer (eT) reaction from the MOF aniline moiety to the adsorbed NR occurs in ~17 ps, inhibiting the ET process between the dye molecules near the MOF surface. This process also was confirmed in Al-ITQ-EB MOF exposed to AN and DMA gas atmospheres, as well as NR in pure aniline. The obtained results demonstrate how modifications in the length and structure of the organic linker in this MOF change the interface interactions and outcome of the photoinduced processes in the composites. Our findings on dye-MOF interface photobehavior are relevant to the design of new materials in which the interface plays a key role in their performance in the fields of catalysis and photonics.

1. INTRODUCTION

In the two past decades, interest in the development of new smart materials has been growing due to the new necessities of the modern society.[1-4] Among these, Metal-Organic Frameworks (MOFs) have become some of the most promising materials due to the variety of possible applications in several fields such as catalysis, photonics and medicine.[5-15] MOFs are formed by multidentate ligands bonded to metal atoms or metal clusters (called also nodes). As a result, these frameworks have remarkable large specific area, distributed along their surface, channels and pores.[16] MOF networks with specific properties are designed in order to control the interactions between the material and guest molecules, and thus the use and performance of the formed composites. By adjusting the linker length in the MOFs, functional groups or the ratio of them, it is possible to modify the intrinsic properties of the material.[16-20]

Recently, a new mesoscopic MOF with lamellar regions (Al-ITQ-HB) has shown promising properties for its use in catalysis.[21] The structural composition of this MOF, formed by aluminium metal clusters and 4-heptylbenzoic acid (HB) as the organic linker, favors the interactions with organic molecules resulting in high reaction yields in aqueous media.[21] Recently, we have reported that specific and non-specific interactions between this MOF and Nile Red (NR) molecules play an important role in the formed composites photobehavior.[22, 23] We have shown that when NR is encapsulated within Al-ITQ-HB, two types of photobehavior were recorded, reflecting location within the framework at different polarities.[22] However, when NR is adsorbed on the same MOF surface, we got a homo energy transfer (ET) between the dye molecules, and we explained the result in terms of different environments created by the metal clusters, spacer linkers and defects.[23]

Here in, to elucidate the importance of the interface of this 2D-MOF when supporting an organic dye, we report studies showing how a change in the linker length

and structure affects the photobehavior of surface-adsorbed molecular probe (NR). The modification of the linker spacer is achieved by replacing the HB chain to either a 4-ethylbenzoic acid (EB) or 4-aminobenzoic acid (AB), giving as a result the Al-ITQ-EB and Al -ITQ-AB MOFs, respectively.[24] Armed with femto- to picosecond (fs-ps) time resolved emission techniques, we interrogate the photo behaviour of the composites. The NR@Al-ITQ-EB ones show a remarkable shorter emission lifetimes (~ 90 ps) than those of NR@Al-ITQ-HB (~220 ps), in addition to faster ET, which is explained in terms of stronger interactions with the Al-oxide clusters of the MOF framework. For NR@Al-ITQ-AB composites, the ET process is inhibited due to a faster (< 17 ps) electron transfer process (eT) from the aniline moiety of the organic linker to the adsorbed dye. This process was experimentally confirmed by exposing the NR@Al-ITQ-EB to aniline and N, N-dimethyl aniline (DMA) atmospheres, observing similar dynamics to that of NR@Al-ITQ-AB. The eT event was also characterized by studying the NR photobehavior dissolved in pure aniline. Furthermore, the ultrafast processes present in the composites were characterized by fs observations time constants of an intramolecular charge transfer (ICT) (~1.2 ps) reaction in all the components. These new results showing the effect of the length and structure of the linker in the MOF on the behaviour of a molecular probe may help in the comprehension and control of the surface properties of these novel materials, opening the way for the development of applications in fields such as catalysis and photonics.

2. EXPERIMENTAL METHODS

2.1 Materials, Synthesis and Characterization of the NR@Al-ITQ MOFs

The materials were prepared (Scheme S1) and characterized (Figure S1) following the procedures reported in the bibliography.[21, 24] In the SI we briefly describe the methods and give the results of the characterization.

For the spectroscopic studies, Nile Red (NR, Sigma-Aldrich, purity >98 %) was adsorbed on the surface of the materials using the following procedure. Firstly, a solution of NR with a known concentration ($1x10^{-3}$M) in dichloromethane (DCM, purchased from Scharlau, spectroscopic grade 99.9%) was prepared. Then, 50 mg of the MOFs were added to 1 mL of the NR/DCM solution, and the mixture was stirred for 24 h at room temperature. Finally, the solvent was eliminated by evaporation. For generating the composites in aniline (Sigma-Aldrich, 99.5%) and N, N-dimethylaniline (DMA, Scharlau, 99%) rich atmospheres, 100 mg of the NR@Al-ITQ-EB composite were put on a watch glass in addition to a container with 10 mL of aniline or DMA which were introduced into a desiccator under vacuum for 24 h.

2.2 Structural, Spectroscopic and Dynamic Measurements

The steady-state UV-visible absorption and fluorescence spectral measurements were carried out using JASCO V-670 and FluoroMax-4 (Jobin-Yvone) spectrophotometers, respectively. The picosecond time-resolved emission experiments have been recorded employing a time-correlated single-photon counting (TSCPC) system. The samples were excited by a 40 ps-pulsed (~1 mW, 40 MHz repetition rate) diode-laser (PicoQuant) centered at 470 nm. The measured instrument response function (IRF) of the set-up is ~70 ps. The fluorescence signal was collected at the magic angle (54.74°), and monitored at a 90° angle to the excitation beam at discrete emission wavelengths. The decays were deconvoluted and fitted to a multiexponential function using the FLUOFIT package (PicoQuant) allowing single and global fits. The quality of the fits as well as the number of exponentials were carefully selected based on the reduced χ^2 values (which were always below <1.2) and the distributions of the residuals. The femtosecond time-resolved emission decays of samples in solid state were collected using a fluorescence up-conversion technique in reflection mode.[22] The system consists of a

Ti:sapphire oscillator (MaiTai HP, Spectra Physics) to generate the excitation beam at 470 nm (~15-20 mW) by second harmonic generation in a BBO crystal. The polarization of the excitation laser was set to the magic angle with respect to the probe beam. The solid sample was placed in a 1-mm-thick randomly moved cell. The fluorescence emission was collected at ~ 0° with respect to the pump laser, focused and gated with the fundamental femtosecond beam (940 nm) to obtain the up-converted signal. The IRF of the apparatus (measured as the reflected signal of the pump signal) was ~300 fs (full width at half-maximum, FWHM) at the excitation wavelength. To analyze the decays, a multi-exponential function convoluted with the IRF was used to fit the experimental data. In all cases, the errors for the calculated time components were smaller than 15%. All the experiments were done at room temperature (295 K).

3. RESULTS AND DISCUSSION

3.1 Steady-State Observations of NR@Al-ITQ-EB and NR@Al-ITQ-AB Composites

To explore the effect of the substituent in the MOF linkers on the photobehavior of an organic molecule located on its surface, we recorded steady-state absorption and emission spectra of the composites formed by the adsorbed NR molecules on the Al-ITQ frameworks of different linkers (Schemes 1 and S1). Figure 1 shows the spectra normalized to the maximum of intensity of NR adsorbed on Al-ITQ-EB and Al-ITQ-AB surfaces in solid state (NR@Al-ITQ-EB and NR@Al-ITQ-AB). Figure S2 exhibits the non-normalized absorption spectra, reflecting a comparable amount of NR in the composites. The structure of Al-ITQ-EB differs from that of Al-ITQ-HB in the length of the alkyl chain of the linker, changing from seven to two carbon atoms (Scheme 1). The absorption spectrum of NR@Al-ITQ-EB shows a broad band (FWHM ~ 6300 cm^{-1}) with maximum of intensity at 552 nm, while the emission band has its maximum of intensity

at ~660 nm. The broadness of the absorption spectrum suggests the presence of different absorbing NR species in the composites. This suggestion is further supported by the dependence of the emission spectra of NR@Al-ITQ-EB on the excitation wavelength (Figure S3), which shifts to higher energies as the excitation wavelength increases. The Stokes shift (2875 cm^{-1}) is similar to the one observed for NR@Al-ITQ-HB (2895 cm^{-1}). Similarly, the FWHM and the shape of both the absorption and emission spectra are also comparable to those of NR@Al-ITQ-HB. We also observe significant spectral overlap between the absorption and emission spectra of NR@Al-ITQ-EB. This behaviour suggest the presence of possible interactions between the NR molecules in their excited states. In a recent study of NR@Al-ITQ-HB composites, we have found similar steady-state photobehavior, which was assigned to homo-energy transfer (ET) between the dye molecules.[23] Thus, expecting similar interactions and processes in the NR@Al-ITQ-EB composites, we suggests a similar explanation. The fluorescence lifetimes and ultrafast dynamics experiments may reveal different interactions of NR with the Al-ITQ-EB frameworks.

Before reporting and analyzing the related experiments, we studied the absorption and emission spectra of NR interacting with a new MOF: Al-ITQ-AB, where the ethyl chain is substituted by an amino group (Scheme S1). The absorption spectrum maximum of the NR@Al-ITQ-AB composite is located at 560 nm with a FWHM of ~5900 cm^{-1}, while the emission spectrum has its maximum of intensity at 645 nm with a narrow shape (FWHM ~1890 cm^{-1}) (Figure 1). However, the emission band is broader at shorter wavelengths (550 – 650 nm) in comparison with the ones of the composites having linkers with alkyl chain substituents, suggesting the presence of relatively more emissive NR species in this spectral region. Additionally, the emission maximum is located at shorter wavelengths (645 nm vs 660 nm), which implies a smaller Stokes shift in comparison

with the other systems (~2200 cm^{-1}), suggesting that a different photoinduced process acting in the NR@Al-ITQ-AB composites. In contrast with the NR@Al-ITQ-EB sample, the emission spectrum does not depend on the excitation wavelength (Figure S3B), also indicating different behaviour and interactions of NR adsorbed on the surface of this MOF associated with the presence of the amino group in the liner (aniline moiety). The excitation spectra of NR interacting on the Al-ITQ MOFs are shown in Figure S4. For NR@Al-ITQ-EB composites the excitation spectra displays similar shape and location to the absorption one, while for NR@Al-ITQ-AB the excitation spectra are narrower in comparison with the absorption one, suggesting the presence of different processes occurring in the excited state.

To better characterize the NR@Al-ITQ-AB photobehavior, we studied the NR@Al-ITQ-EB composites exposed to aniline (AN) and N, N-dimethylaniline (DMA) gas atmospheres. Scheme 2 illustrates the idea and expected formed composites (NR@Al-ITQ-EB/AN and NR@Al-ITQ-EB/DMA) under these conditions. Figure 1 shows a comparison of the UV-visible absorption and emission spectra of NR@Al-ITQ-EB, NR@Al-ITQ-AB and NR@Al-ITQ-EB/DMA. The exposed composites show a broad absorption bands with a maximum of intensity at ~553 nm, which does not differ from the NR@Al-ITQ-AB one (Figures 1 and S5). However, the FWHM (~8630 cm^{-1}) of the band is significantly larger than the ones obtained for the samples without the presence of AN or DMA, which indicates the existence of additional species in the ground state. The emission spectra show a narrow band with similar shape to the ones for the other composites, but with the maximum of emission intensity located at 657 nm. The location of this emission band falls between those of the NR@Al-ITQ-AB and NR@Al-ITQ-EB ones, which suggests that AN and DMA atmospheres have affected a population

of the NR molecules in the composites using Al-ITQ-EB, and thus resulting in a behaviour similar to the one for NR located on the surface of the Al-ITQ-AB framework.

To provide more knowledge on the effect of the aniline moiety in NR@Al-ITQ-AB on NR spectroscopy, we studied the behaviour of the dye in pure aniline. Figure S6 shows the UV-visible absorption and emission spectra of the sample. The absorption spectrum is composed by a band with a maximum at 564 nm and a much narrower shape (FWHM ~2970 cm^{-1}) than the ones obtained for the composites. The narrowing of the absorption band reflects a higher homogeneity of NR populations than in the composites. The emission band is located at 639 nm and it also has very narrow shape (FWHM ~1260 cm^{-1}). The location of the bands are similar to the ones of the NR@Al-ITQ-AB composite (560 and 645 nm for the absorption and emission respectively).

3.2 Picosecond Time-Resolved Fluorescence Experiments

3.2.1 NR@Al-ITQ-EB Composites

To elucidate how the surface of the studied MOF structures affects the photodynamics of adsorbed NR molecules, we carried out time-resolved emission experiments with picosecond resolution in the solid state. Table 1 shows the values of the lifetimes, and the pre-exponential factors and contributions (normalized to 100), obtained from the multiexponential fit of representative six emission decays of the composites upon excitation at 470 nm. To begin with, Figure 2A exhibits the decays of NR@Al-ITQ-EB at different observation wavelengths, while Table S1 shows the values obtained from the multiexponential fit for all the emission decays. To obtain an accurate fit, we used a tri-exponential function, with values of τ_1 = 0.09 ns, τ_2 = 0.93 ns and τ_3 = 2.59 ns. These components are slightly faster but comparable to those observed for the NR@Al-ITQ-HB composite (0.22, 1.33 and 3.61 ns) having comparable amounts of adsorbed NR.[23] Thus,

we assign the component having the shortest time (0.09 ns), and which decays at shorter wavelengths and rises at longer ones, to the homo ET process between the adsorbed NR molecules. In a previous work, we have demonstrated that the time of this event depends on the concentration of the adsorbed NR molecules.[23] In the present composites, the shortening in the alkyl chains length (from 7 to 2 carbon atoms) implies a higher proportion of metal (Al-oxide) clusters in comparison with the organic linkers (Scheme 1). Thus, this fact produces a more polar environment around the adsorbed NR, and therefore change in its photodynamics. This change is translated in a faster ET reaction between the NR molecules. In agreement with our previous report, we assign the intermediate time constant (0.93 ns) to the emission of aggregated species formed by NR molecules and which do not undergo the ET process. The longest component (2.59 ns) is assigned to the emission of the species formed as result of the ET process. Scheme 3A summarized the above assignment of the times related to the emission decays of NR molecules directly interacting with the MOF surface. Considering the used NR concentration (10^{-3} M) to make the composites, the dye molecules may form several layers on the surface of the MOF (Scheme 2A). Some of these molecules (those located far from the MOF surface) will not be affected significantly by the conditions of the MOF surface, and therefore their population may not undergo ET event. In a previous study, we have observed a component of ~0.3 ns assigned to the relaxation of the local excited (LE) state.[23] However, in the present work, this component is not observed probably due to the proximity of the values of the shortest and intermediate times.

In order to get further understanding of the photobehavior of the NR@Al-ITQ-EB composites, we collected its picosecond Time-Resolved Emission Spectra (TRES). Figures 2C and S7A show respectively, the normalized and non-normalized TRES, upon excitation at 470 nm and gating at different delay times. We distinguish two features: (i)

the spectra display a band (in early-time tail) between 575 and 675 nm, and which intensity decreases to ~50% at ~500 ps, while (i i) the relative intensity of the main band with maximum at ~675 nm increases within the same time. The TRES evolution of NR@Al-ITQ-EB is comparable with the NR@Al-ITQ-HB one,[23] but with a smaller shift of the bands at the bluest part, in agreement with the faster ET process in the present composites. Thus, we assign the emission at 550-675 nm to that of NR species undergoing ET and of aggregates. The band having the maximum of intensity at 675 nm, and living longer is due to species formed after an ET process on MOF surface.

3.2.2 NR@Al-ITQ-AB composites

Figure 2B shows the emission decays of the NR@Al-ITQ-AB composite collected at different observation wavelengths, and Tables 1 and S2 give the parameters obtained from the multiexponential fit of the decays. The fit gives values of τ_1 = 0.13, τ_2 = 0.54 and τ_3 = 2.10 ns. The decays are shorter (done at ~3 ns), and in contrast with the NR@ Al-ITQ-HB and NR Al-ITQ-EB composites, for the NR@ Al-ITQ-AB ones all the components decay along the whole studied spectral range with constant contributions of ~69 %, ~25 % and ~6 %, respectively. Compared to NR@Al-ITQ-EB, the contribution (c_3) of the longest component at the reddest part of the emission spectra strongly decreases from ~70% to ~5%, suggesting that the channel (ET) giving rise to these species is not as efficient as in NR@Al-ITQ-EB composites (Table 1). Interestingly, in this sample we observed no rise component, which suggests that either the ET process is not occurring in these composites, or it is too fast to be recorded with the resolution of our system (IRF ~70 ps). To explain the observed behaviour, we consider that the interactions of NR with the surface of this MOF surface are stronger than with Al-ITQ-EB ones due to the presence of amino groups in Al-ITQ-AB. These groups can interact with NR molecules by either forming H-bonding complexes or through photoinduced electron transfer

process from the aniline moiety of the MOF to NR, thus opening new decay pathways for the excited interacting populations. In a study on the H-bonding interactions of NR with the surrounding solvent molecules, it has been shown that the fluorescence lifetimes and the quantum yield decrease as the H-bonding character of the medium increase enhancing the efficiency of non-radiative decay channels.[25] Thus, the specific interactions of NR with aniline moiety of Al-ITQ-AB could inhibit the homo ET process, which happened in ~90 ps in NR@Al-ITQ-EB, by promoting other faster dynamics and accelerating the decay of the NR populations. On the other hand, for organic molecules with comparable structures to NR (for example oxazine derivatives), emission quenching due to a photoinduced electron transfer (eT) from aniline derivatives that act as donors has been reported.[26, 27] In these systems, the eT happens in femtosecond regime. The occurrence of eT reaction could also explain why the ET process is not observed in the Al-ITQ-AB composite. Femtosecond experiments will clarify the photoinduced processes that NR is undergoing in the composites.

To get a spectral and dynamical picture, Figures 2D and S7B show the normalized and non-normalized TRES of NR@Al-ITQ-AB, respectively. Unlike the previously discussed cases, the result here allows two observations: (i) a weak variation of the TRES shape with the gating time, which is in agreement with the decays in Figure 2B, and reflecting the lack of ET process in NR molecules interacting with the aniline moiety of the MOF. (i i) The intensity maximum is now at ~650 nm, different from the 675 nm of the NR@Al-ITQ-EB, also indicating the emission from NR species produced by ET is not relevant.

3.2.3 NR@Al-ITQ-EB Composites Interacting with AN and DMA Atmospheres

To experimentally prove the occurrence of eT in the NR@Al-ITQ-AB, we performed picosecond experiments on NR@Al-ITQ-EB interacting with gas phase of aniline (AN) and N, N-dimethylaniline (DMA) (Scheme 2B). We examine first the effect of aniline atmosphere We refer to this sample as NR@Al-ITQ-EB/AN. Figure S8 shows the recorded emission decays and Table S3 exhibits the time values and related parameters obtained from multiexponential fits. To accurately fit the decays, we used a triexponential function with time constants of τ_1 = 0.11, τ_2 = 0.55 and τ_3 = 2.31 ns. Contrary to the behaviour of NR@Al-ITQ-EB, for NR@Al-ITQ-EB/AN we observed no rising component assigned to the ET process in the former. This is a direct evidence that aniline moiety quenches the emission of adsorbed NR on this moiety and the faster quenching in NR@Al-ITQ-AB has its origin in an efficient eT from the aniline moiety in the MOF to adsorbed NR molecules (Scheme 2). NR in pure aniline solution gives a monoexponential emission decay of ~20 ps (Figure S9). This is confirmed by fs-experiments (see below). Note also, the obtained lifetimes of NR@Al-ITQ-EB interacting with aniline atmosphere are comparable to the ones observed for the NR@Al-ITQ-AB composites (0.13, 0.54 and 2.10 ns).

The behaviour of the NR@Al-ITQ-EB composite was also studied by carrying out the same experiment but replacing the AN atmosphere by a DMA one (Scheme 2B). The main difference between AN and DMA abilities is that the former can act as H-bonding donor system, while the DMA cannot. Figure 2E shows a comparison of the emission decays of the different composites studied in this work collected at 725 nm, where the signal are more affected by the MOF surface, and Table1 gives the relevant parameters for the NR@Al-ITQ-EB/DMA composites obtained from the

multiexponential fit. All recorded decays and their fitting parameters are shown in Figure S10 and Table S4. For NR@Al-ITQ-EB/DMA, we obtained components of 0.15, 0.71 and 2.25 ns. These values are very similar to those obtained for NR@Al-ITQ-EB/AN (0.11, 0.55 and 2.3 ns), which suggests that the ET inhibition in the NR@Al-ITQ-AB composite photobehavior is not a result of H-bonding interactions between the NR molecules and the aniline moiety of the MOF linkers, but rather by a direct eT not involving H-bondings at the surface of the MOF. We note that the DMA atmosphere has affected the NR dynamics when it is adsorbed on Al-ITQ-EB surface, showing a behaviour similar to the one observed for NR molecules located on the Al-ITQ-AB surface (Figure 2E). Thus, if we consider the adsorption of the NR molecules on the MOF surface as a multilayer system (Scheme 2B), and assuming that the diffusion of the DMA molecules through the NR levels will not be highly efficient, the upper layers of NR will be more affected by the DMA atmosphere and will most likely behave in similar way as the NR@Al-ITQ-AB composite providing a direct interaction with the aniline moiety, and therefore, undergoing the eT reaction. On the other hand, we expect that some populations closer to the MOF surface of Al-ITQ-EB and to which DMA molecules have not access, will not undergo eT. In short, the NR@Al-ITQ-EB/DMA shows a behavior which is an average of the dynamics of NR molecules affected and not affected by DMA presence. Therefore, the emission decay of NR@Al-ITQ-EB/DMA composites is a combination of those shown by NR@Al-ITQ-EB (no eT) and NR@Al-ITQ-AB (strong eT) (Figure 2E).

The obtained three components in the emission signals of NR@Al-ITQ-AB and NR@Al-ITQ-EB/DMA are present as decays along the whole studied emission range and, considering the proposed multilayer NR@MOF scheme (Scheme 2), they are the result of a combination of NR molecules on and far from the MOF surfaces. Thus, we

suggest that the shortest components in both, the NR@Al-ITQ-AB (0.13 ns, Scheme 3B) and NR@Al-ITQ-EB/DMA (0.15 ns), correspond to the emission of NR molecules from the charge separated (CS) state generated after the ICT reaction in NR not in direct contact with the MOF surface. In both cases, the intermediate component (0.54 and 0.71 ns, respectively) is assigned to the emission of NR aggregates. Notably, the value of the time of this component for the NR@Al-ITQ-EB/DMA composite (0.71 ns) is an average of the ones obtained for NR@Al-ITQ-EB (0.93 ns) and NR@Al-ITQ-AB (0.54 ns) composites. Finally, the longest component for the NR@Al-ITQ-EB/DMA composites has similar value of the emission lifetime (2.25 ns) and behaviour to the resulting ET species in the NR@Al-ITQ-EB composites (Table 1). This component is probably produced by NR molecules located closer to the MOF surface, in agreement with previous reports.[23] However, for the NR@Al-ITQ-AB, the τ_3-component has the lowest contribution in the emission signal (Table 1). Interestingly, the eT event in the NR@Al-ITQ-AB composites can be used to develop optoelectronic devices based on ultrafast charge separation, like for example a photovoltaic cells or photodetectors. One can combine several strongly absorbing dyes in the visible-IR regions and this kind of MOFs.

3.3 Femtosecond Experiments

To get a further and deeper understanding of the photobehavior of the composites at very short time regime, femtosecond (fs) emission experiments were carried out. Figures 3 and 4 show the transient decays of the 3 composites upon fs-excitation at 470 nm. Tables 2-4 give the parameters obtained from the fit of the recorded transients. The value of the longest component in the emission decays of all the studied samples was fixed in the fits, using the one obtained from the picosecond experiments. For the NR@Al-ITQ-EB composites, we got three components of ~1.2, ~87 ps and 2.59 ns. The two first components decay at the green side of the emission spectra and rise from 615

nm to the end of the observation range, which indicates the presence of two different processes occurring in the excited state of the composites. The ~87 ps component was assigned from the picosecond experiments to the ET. It is worth noting that the NR emission from the CS state has similar lifetime to the ET species, resulting in a component with a value that is an average of both emitters (Scheme 3A). We assign the shortest component (~1.2 ps) to the ICT. This time is longer than the one obtained for the NR@Al-ITQ-HB composite (~0.5 ps).[23] We explain this difference in terms of a change in the strength of the interactions of NR molecules with the framework. As we explained in the ps-part, the shortening in the alkyl chain (from 7 to 2 carbon atoms) makes the adsorbed NR molecules under a stronger environment of the Al-oxide nodes. This polar environment will influence the stability and dynamics of the initially excited adsorbed NR. Thus, the interaction with the Al-ITQ-EB will stabilize the locally excited state of the dye, which increases the energy barrier for the ICT process to occur, and therefore the process becomes longer.

Femtosecond transients at NR@Al-ITQ-AB composites revealed the presence of two components in addition to those of hundreds of ps. The obtained time values were ~1, ~17, ~ 115 and 540 ps (Table 3). In contrast with the previous composites, and in agreement with the picosecond observations, only the component of ~1 ps behaves as a rise, which we assign to the ICT process. The rising behaviour precludes to attribute it to an eT event from the AN moiety, as this process normally leads to no fluorescent species.[26, 27] Note also that this component becomes slightly shorter in comparison with the NR@Al-ITQ-EB one (1.2 ps), which reflects a higher polarity of the environment created by the presence of the amino linkers. The component of 17 ps, which has not been observed in the previous composites, is assigned to the emission of a NR species quenched due to its interaction with the AN moiety. It has been reported that the

interaction of similar organic dyes with aniline derivatives produces a strong quenching of the emission of these molecules due to the transfer of an electron from these AN systems to the excited dyes.[26] This eT reaction occurs in the ultrafast scale, therefore it is probably occurring in NR@Al-ITQ-AB sample in ~17 ps (Scheme 3B). Finally, the component of ~115 ps is due to the NR aggregates emission, as we attributed it was assigned in the ps-experiments.

When the NR@Al-ITQ-EB/DMA composite was studied with fs-resolution, we observed a behaviour similar to the NR@Al-ITQ-AB composite (Figure 4B). The transients are composed of three components having time constants of ~1.4, ~16 ps, and the fixed one of 2.25 ns (Table 4). Following our previous explanation, the shortest component is attributed to the ICT process. This value is probably affected by the ~16 ps decay component, which is translated in a small increment of this shortest component in comparison with the one observed for the NR@Al-ITQ-EB complex. Interestingly, the ~16 ps component is observed in the NR@Al-ITQ-EB/DMA transients, but absent in those of the same composite without being not exposed to the DMA gas atmosphere. This component is recorded also in the NR@Al-ITQ-AB transients, confirming that it reflects the interaction with the AN moieties of the MOF.

Finally, to strength our assignment given for the recorded behaviour, NR/aniline (solution) was also studied with femtosecond resolution. Figure S11 shows the recorded transients, and Table S5 gives the obtained parameters from the fits. The system decays with lifetimes of ~1.1 and ~17 ps. The shortest time value is assigned to the ICT process, which in this case shows similar value to the one observed for the NR@Al-ITQ-AB system. The presence of the ~17 ps component confirms the assignment of this time to the deactivation of NR due to the eT process. The high contribution of this component from 600 to 650 nm of observation wavelength, suggests the strong effect that the

interaction between NR and the aniline has on the dye photobehavior. The eT process inhibits the ET reaction in both systems, the NR@Al-ITQ-AB and NR@Al-ITQ-EB/DMA, resulting in the different photobehavior observed in comparison with NR@Al-ITQ-EB and NR@Al-ITQ-HB composites.

Table 5 shows a summary of the characterized processes in the studied composites. It is clear that the length and structure of the linker in the MOF strongly affect the energy and electron transfer events, being the latest dominantly the former in NR@Al-ITQ-AB composites. The shortening in the chain produces a shortening in the ET process, which is explained in terms stronger interactions with the framework due to the higher polarity of the environment provided by the Al-oxide clusters. This change explains also the difference in the ICT process time, as those interactions produces a stabilization in the LE state. The presence of the aniline moiety implies different dynamics, with the absence of the ET process but the dominance of the eT reaction. This explanation is strongly supported when exposing the NR@Al-ITQ-EB composite to AN and DMA gas atmosphere, as well as when studying NR in pure AN solution.

4. CONCLUSIONS

In this work, we have shown how a change in the linker length and structure of the Al-ITQ MOFs conditions the interactions between the framework and an organic dye, the NR, located on its surface and, therefore its dynamics. The NR@Al-ITQ-EB composites show the presence of an ET event (~ 90 ps) between the NR molecules located on the MOF surface, and which is faster than that occurring in NR@Al-ITQ-HB where the aliphatic chain of the linker is formed by seven carbons instead of two. The speeding up of the process reflects a stronger interaction between the NR molecules due to a higher polarity produced by the MOF surface structure in which the apolar environment is reduced. We also observed decaying components having time constants of 0.93 and 2.59

ns, assigned respectively to aggregates emission and the resulting ET species. These values are also shorter to those observed in NR@Al-ITQ-HB, reflecting the effect of chain length in the photobehavior of NR when interacting with this MOF surface. On the other hand, when the linker contains an aniline moiety (Al-ITQ-AB), the ET process is inhibited due to a faster eT reaction from the MOF to the NR molecules. The occurrence of this eT process on the surface was confirmed by studying the NR@Al-ITQ-EB composites exposed to AN- and DMA-rich gas atmospheres, as well as observing the photobehavior of NR in pure aniline solution. In all the composites, femtosecond experiments reveal a photoinduced ICT process (~1.2 ps) in adsorbed NR. For NR@Al-ITQ-AB, in addition to the decay times observed in the ps-experiments, we also recorded a short lifetime of ~17 ps assigned to NR adsorbed structures, which experience an eT process. Thus, we can conclude that when the substituent in the linker of the MOF is a non-interactive group, such as an aliphatic chain, the photobehavior of the composites is dominated by the interaction between the adsorbed dye molecules, and the effect of the length is reflected in the time constant of the ET process. However, when the substituent is an aniline moiety, the homo ET process is blocked, and an eT reaction with the framework becomes the dominant driving force in the photoinduced dynamics of NR. This event at the surface of the MOF generates positive and negative charges which might be used for a propose in a photonic device like photodetectors or solar cells. These new insights highlight the power and versatility of this MOF, turning it into a great candidate to be used not only in catalysis, but also in photonics of composites, where the interactions between the host and the guest is paramount to its stability and performance.

ASSOCIATED CONTENT

Supporting Information

Scheme S1: synthetic pathway and resulting framework of the used MOFs. Figure S1: XRD, TG, DTA and TEM images of Al-ITQ-EB and Al-ITQ-AB. Figure S2: UV-visible absorption spectra of NR@Al-ITQ-HB, NR@Al-ITQ-AB and NR@Al-ITQ-EB. Figures S3 and S4: emission and excitation spectra of NR@Al-ITQ-EB and NR@Al-ITQ-AB. Figure S5: Steady-state spectra of NR@Al-ITQ-EB/aniline. Figure S6: Steady-state spectra of NR /aniline. Figure S6: Figure S7: TRES of NR@Al-ITQ-EB and NR@Al-ITQ-AB. Tables S1-S4: Lifetimes, pre-exponential factors and contributions obtained from the decays analysis of NR@Al-ITQ-EB, NR@Al-ITQ-AB, NR@Al-ITQ-EB/aniline and NR@Al-ITQ-EB/DMA. Figures S8-S10: Normalized magic-angle emission decays of NR@Al-ITQ-EB/aniline, NR/aniline and NR@Al-ITQ-EB/DMA. Figure S11: Femtosecond emission transients of NR/aniline. Table S5: Values of the time constants and normalized (to 100) pre-exponential factors (ai) obtained from the transients of NR/aniline.

AUTHOR INFORMATION

Corresponding Author:

*Email: Abderrazzak.Douhal@uclm.es

Author Contributions

The MOFs and their composites were made and characterized by the ITQ group. The spectroscopic experiments were executed and analyzed by the UCLM group. The manuscript was written through contributions of all authors. All authors have given approval to the final version of the manuscript.

Notes

The authors declare no competing financial interest.

ACKNOWLEDGEMENTS,

This work was supported by MINECO through projects MAT2014-57646-P, MAT2017-86532-R and MAT2017-82288-C2-1-P. J.M.M. thanks the predoctoral fellowship from the Severo Ochoa program for support (SEV-2016-0683) and E.C.M thanks the MINECO for the FPI fellowship (BES-2015-071495). We thank Dr. John Spencer Baskin for reading the manuscript.

REFERENCES

1. Alarcos, N.; Cohen, B.; Ziółek, M.; Douhal, A., Photochemistry and Photophysics in Silica-Based Materials: Ultrafast and Single Molecule Spectroscopy Observation. *Chem. Rev.* **2017,** *117*, 13639-13720.
2. Kaskel, S., Porous Metal-Organic Frameworks. In *Handbook of Porous Solids*, Wiley-VCH Verlag GmbH: 2008; pp 1190-1249.
3. Kitagawa, S.; Kitaura, R.; Noro, S.-i., Functional Porous Coordination Polymers. *Angew. Chem. Int. Ed.* **2004,** *43*, 2334-2375.
4. Rowsell, J. L. C.; Yaghi, O. M., Metal–Organic Frameworks: A New Class of Porous Materials. *Microporous Mesoporous Mater.* **2004,** *73*, 3-14.
5. Czaja, A. U.; Trukhan, N.; Muller, U., Industrial Applications of Metal-Organic Frameworks. *Chem. Soc. Rev.* **2009,** *38*, 1284-1293.
6. Getman, R. B.; Bae, Y. S.; Wilmer, C. E.; Snurr, R. Q., Review and Analysis of Molecular Simulations of Methane, Hydrogen, and Acetylene Storage in Metal-Organic Frameworks. *Chem. Rev.* **2012,** *112*, 703-723.
7. Li, B.; Wen, H. M.; Wang, H.; Wu, H.; Tyagi, M.; Yildirim, T.; Zhou, W.; Chen, B., A Porous Metal-Organic Framework with Dynamic Pyrimidine Groups Exhibiting Record High Methane Storage Working Capacity. *J. Am. Chem. Soc.* **2014,** *136*, 6207-6210.
8. Li, J.-R.; Kuppler, R. J.; Zhou, H.-C., Selective Gas Adsorption and Separation in Metal-Organic Frameworks. *Chem. Soc. Rev.* **2009,** *38*, 1477-1504.
9. Murray, L. J.; Dinca, M.; Long, J. R., Hydrogen Storage in Metal-Organic Frameworks. *Chem. Soc. Rev.* **2009,** *38*, 1294-1314.
10. Ma, L.; Abney, C.; Lin, W., Enantioselective Catalysis with Homochiral Metal-Organic Frameworks. *Chem. Soc. Rev.* **2009,** *38*, 1248-1256.
11. Liu, J.; Chen, L.; Cui, H.; Zhang, J.; Zhang, L.; Su, C.-Y., Applications of Metal-Organic Frameworks in Heterogeneous Supramolecular Catalysis. *Chem. Soc. Rev.* **2014,** *43*, 6011-6061.
12. Li, J.-R.; Sculley, J.; Zhou, H.-C., Metal–Organic Frameworks for Separations. *Chem. Rev.* **2012,** *112*, 869-932.

13. Horcajada, P.; Gref, R.; Baati, T.; Allan, P. K.; Maurin, G.; Couvreur, P.; Férey, G.; Morris, R. E.; Serre, C., Metal–Organic Frameworks in Biomedicine. *Chem. Rev.* **2012,** *112*, 1232-1268.
14. Kurmoo, M., Magnetic Metal-Organic Frameworks. *Chem. Soc. Rev.* **2009,** *38*, 1353-1379.
15. Foster, M. E.; Azoulay, J. D.; Wong, B. M.; Allendorf, M. D., Novel Metal-Organic Framework Linkers for Light Harvesting Applications. *Chem. Sci.* **2014,** *5*, 2081-2090.
16. Li, M.; Li, D.; O'Keeffe, M.; Yaghi, O. M., Topological Analysis of Metal-Organic Frameworks with Polytopic Linkers and/or Multiple Building Units and the Minimal Transitivity Principle. *Chem. Rev.* **2014,** *114*, 1343-1370.
17. Lu, W.; Wei, Z.; Gu, Z.-Y.; Liu, T.-F.; Park, J.; Park, J.; Tian, J.; Zhang, M.; Zhang, Q.; Gentle Iii, T.; Bosch, M.; Zhou, H.-C., Tuning the Structure and Function of Metal-Organic Frameworks Via Linker Design. *Chem. Soc. Rev.* **2014,** *43*, 5561-5593.
18. Getman, R. B.; Bae, Y.-S.; Wilmer, C. E.; Snurr, R. Q., Review and Analysis of Molecular Simulations of Methane, Hydrogen, and Acetylene Storage in Metal–Organic Frameworks. *Chem. Rev.* **2012,** *112*, 703-723.
19. Wilmer, C. E.; Leaf, M.; Lee, C. Y.; Farha, O. K.; Hauser, B. G.; Hupp, J. T.; Snurr, R. Q., Large-Scale Screening of Hypothetical Metal–Organic Frameworks. *Nature Chemistry* **2011,** *4*, 83.
20. Martin, R. L.; Lin, L.-C.; Jariwala, K.; Smit, B.; Haranczyk, M., Mail-Order Metal–Organic Frameworks (Mofs): Designing Isoreticular Mof-5 Analogues Comprising Commercially Available Organic Molecules. *J. Phys. Chem. C* **2013,** *117*, 12159-12167.
21. García-García, P.; Moreno, J. M.; Díaz, U.; Bruix, M.; Corma, A., Organic–Inorganic Supramolecular Solid Catalyst Boosts Organic Reactions in Water. *Nat. Commun.* **2016,** *7*, 10835-10843.
22. Caballero-Mancebo, E.; Cohen, B.; Moreno, J. M.; Corma, A.; Díaz, U.; Douhal, A., Exploring the Photodynamics of a New 2d-Mof Composite: Nile Red@Al–Itq-Hb. *ACS Omega* **2018,** *3*, 1600-1608.
23. Caballero-Mancebo, E.; Moreno, J. M.; Corma, A.; Díaz, U.; Cohen, B.; Douhal, A., How Does the Surface of Al–Itq-Hb 2d-Mof Condition the Intermolecular Interactions of an Adsorbed Organic Molecule? *ACS Applied Materials & Interfaces* **2018,** *10*, 20159-20169.
24. Moreno, J. M.; Velty, A.; Vidal-Moya, J. A.; Diaz, U.; Corma, A., Growth-Modulating Agents for the Synthesis of Al-Mof-Type Materials Based on Assembled 1d Structural Subdomains. *Dalton Transactions* **2018,** *47*, 5492-5502.
25. Cser, A.; Nagy, K.; Biczók, L., Fluorescence Lifetime of Nile Red as a Probe for the Hydrogen Bonding Strength with Its Microenvironment. *Chem. Phys. Lett.* **2002,** *360*, 473-478.
26. Kumpulainen, T.; Lang, B.; Rosspeintner, A.; Vauthey, E., Ultrafast Elementary Photochemical Processes of Organic Molecules in Liquid Solution. *Chem. Rev.* **2017,** *117*, 10826-10939.
27. Yoshihara, K., *Advances in Chemical Physics: Electron Transfer—from Isolated Molecules to Biomolecules.* Wiley Online Library: 2007; Vol. 107.

FIGURES AND TABLES

Figure 1. Normalized steady-state UV-visible absorption and emission spectra (upon excitation at 470 nm) of (1) NR@Al-ITQ-AB, (2) NR@Al-ITQ-EB and (3) NR@Al-ITQ-EB/DMA in solid state. The emission spectra of (1) and (3) are normalized to (2) by multiplying by 3.2 and 2.1, respectively. The inserted pictures are of the illuminated composites under the 365 nm UV lamp irradiation.

Figure 2. Normalized magic-angle emission decays and Time-Resolved Emission Spectra of (A and C) NR@Al-ITQ-EB and (B and C) NR@Al-ITQ-AB upon excitation at 470 nm. The observation wavelengths for A and B were 575, 600, 625, 650, 675, 700, 725, 750 and 775 nm. The inserts of A and B show a zoom of the emission decays; while those of C and D give the gating time after the laser excitation. (E) Comparison of the emission decays at 725 nm of the excited (470 nm) composites of NR interacting with Al-ITQ-HB, Al-ITQ-EB, Al-ITQ-EB/DMA and Al-ITQ-AB MOF surfaces.

Figure 3. Femtosecond emission transients of (A) NR@Al-ITQ-EB, (B) NR@Al-ITQ-AB and (C) NR@Al-ITQ-EB/DMA in solid state upon excitation at 470 nm and observation at the indicated wavelengths. The solid lines are from the best fits using a multiexponential function. IRF is the instrument response function of the fs-set up (~300 fs).

Figure 4. Comparison of the fs-transients at short and long emission wavelength of observation for (A) NR@Al-ITQ-EB, (B) NR@Al-ITQ-AB and (C) NR@Al-ITQ-EB/DMA in solid state upon excitation at 470 nm and observation at 575 and 655 nm. The solid lines are from the best fits using a multiexponential function.

Scheme 1. Cartoon (not in scale) illustrating the adsorption of Nile Red (NR) on the Al-ITQ-HB and Al-ITQ-EB surface. The distance between the Al-oxide clusters was estimated in ref. 24.

Scheme 2. Illustration (not in scale) of a proposed multilayer scenario of the composites formed by (A) NR distributed along the Al-ITQ-EB and (B) when the composites are exposed to AN/DMA atmosphere. The NR molecules located close to the MOF surface are affected by its environment, while those at the upper layers are (A) not affected by the MOF or (B) mostly affected by the AN/DMA molecules.

Scheme 3. Photodynamic schemes of (A) NR@Al-ITQ-EB and (B) NR@Al-ITQ-AB composites. LE, ICT, CS, ET and eT mean local excited state, intramolecular charge transfer, charge separated state, energy transfer and electron transfer, respectively. See text for details.

Table 1. Values of the lifetimes, their pre-exponential factors (a_i) and contributions (c_i) normalized to 100 of the used composites upon excitation at 470 nm.

Table 2. Values of the time constants and normalized (to 100) pre-exponential factors (ai) obtained from a multiexponential fit of the femtosecond emission transients of solid NR@Al-ITQ-EB upon excitation at 470 nm, and observation as indicated. The negative sign for a_i indicates a rising component in the emission signal.

Table 3. Values of the time constants and normalized (to 100) pre-exponential factors (ai) obtained from a multiexponential fit of the femtosecond emission transients of NR@Al-ITQ-AB upon excitation at 470 nm, and observation as indicated. The negative sign for a_i indicates a rising component in the emission signal.

Table 4. Values of the time constants and normalized (to 100) pre-exponential factors (ai) obtained from a multiexponential fit of the femtosecond emission transients of

NR@Al-ITQ-EB/DMA composites upon excitation at 470 nm, and observation as indicated. The negative sign for a_i indicates a rising component in the emission signal.

Table 5. Comparison of the time constants of ICT, ET and eT events studied in the present composites and NR in AN solution.

Figure 1:

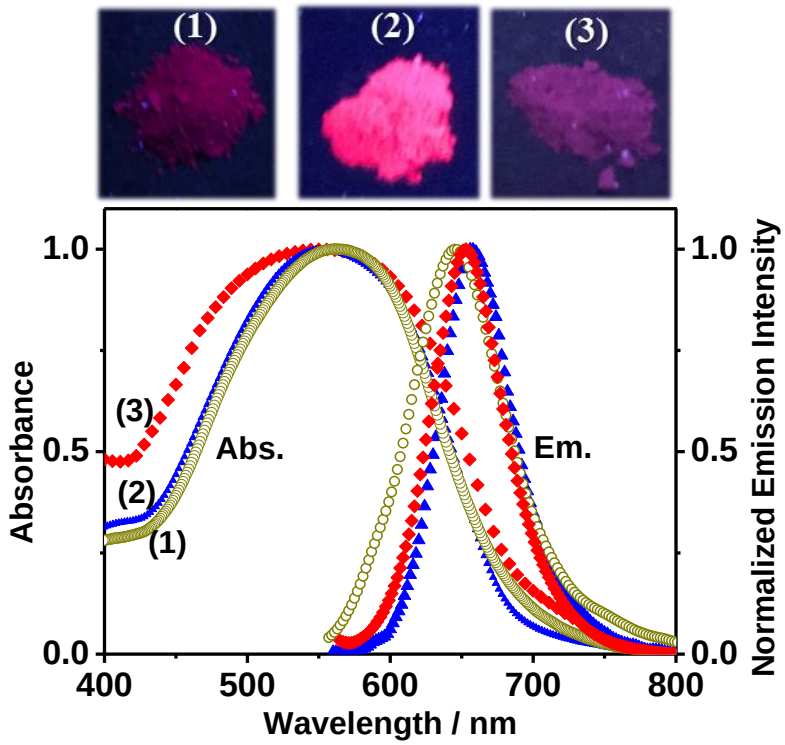

Figure 2:

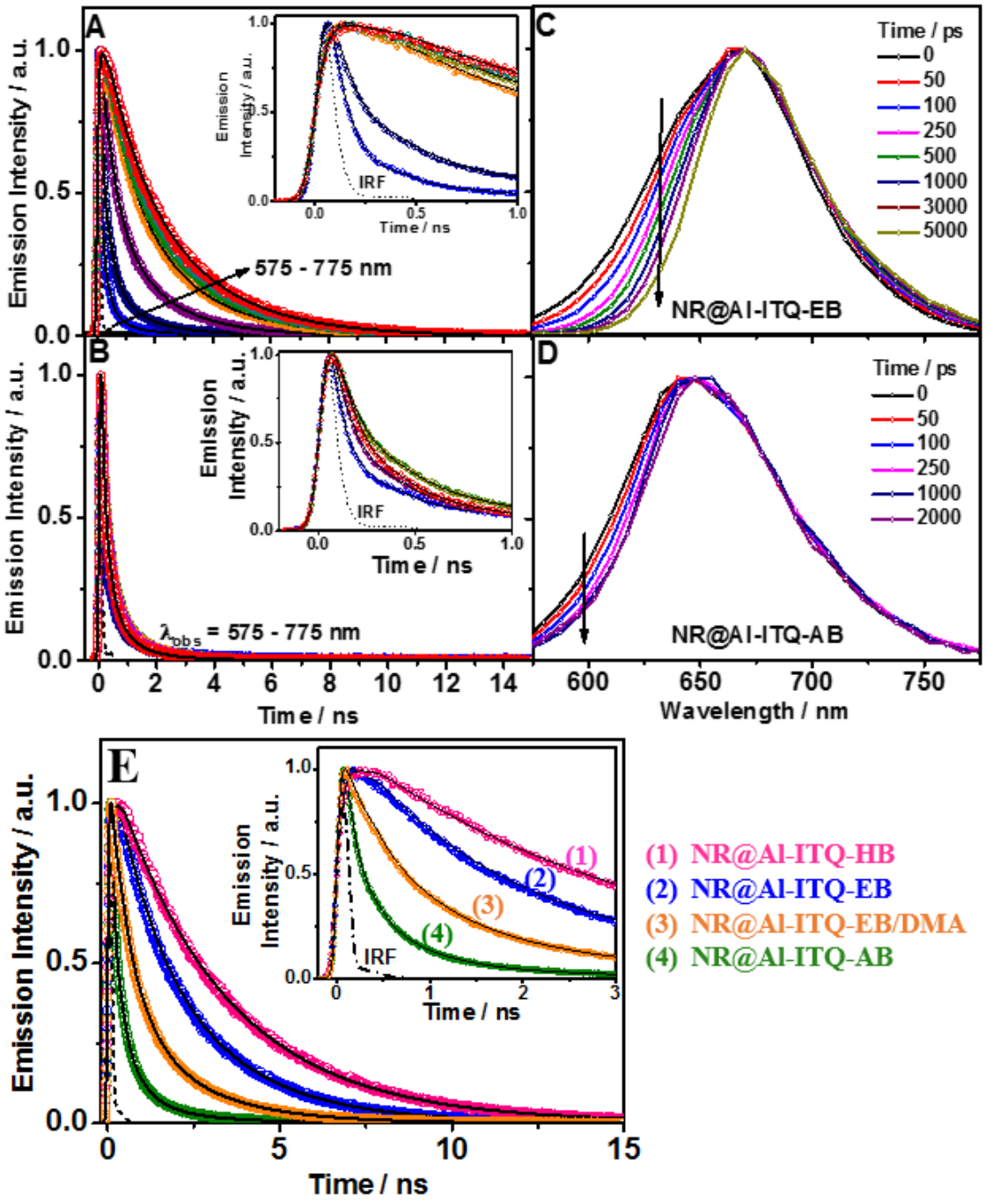
A
B
C
D
E
Emission Intensity / a.u.
Time / ns
IRF
575 - 775 nm
λobs = 575 - 775 nm
Time / ps
0
50
100
250
500
1000
3000
5000
2000
NR@Al-ITQ-EB
NR@Al-ITQ-AB
Wavelength / nm
(1) NR@Al-ITQ-HB
(2) NR@Al-ITQ-EB
(3) NR@Al-ITQ-EB/DMA
(4) NR@Al-ITQ-AB

Figure 3:

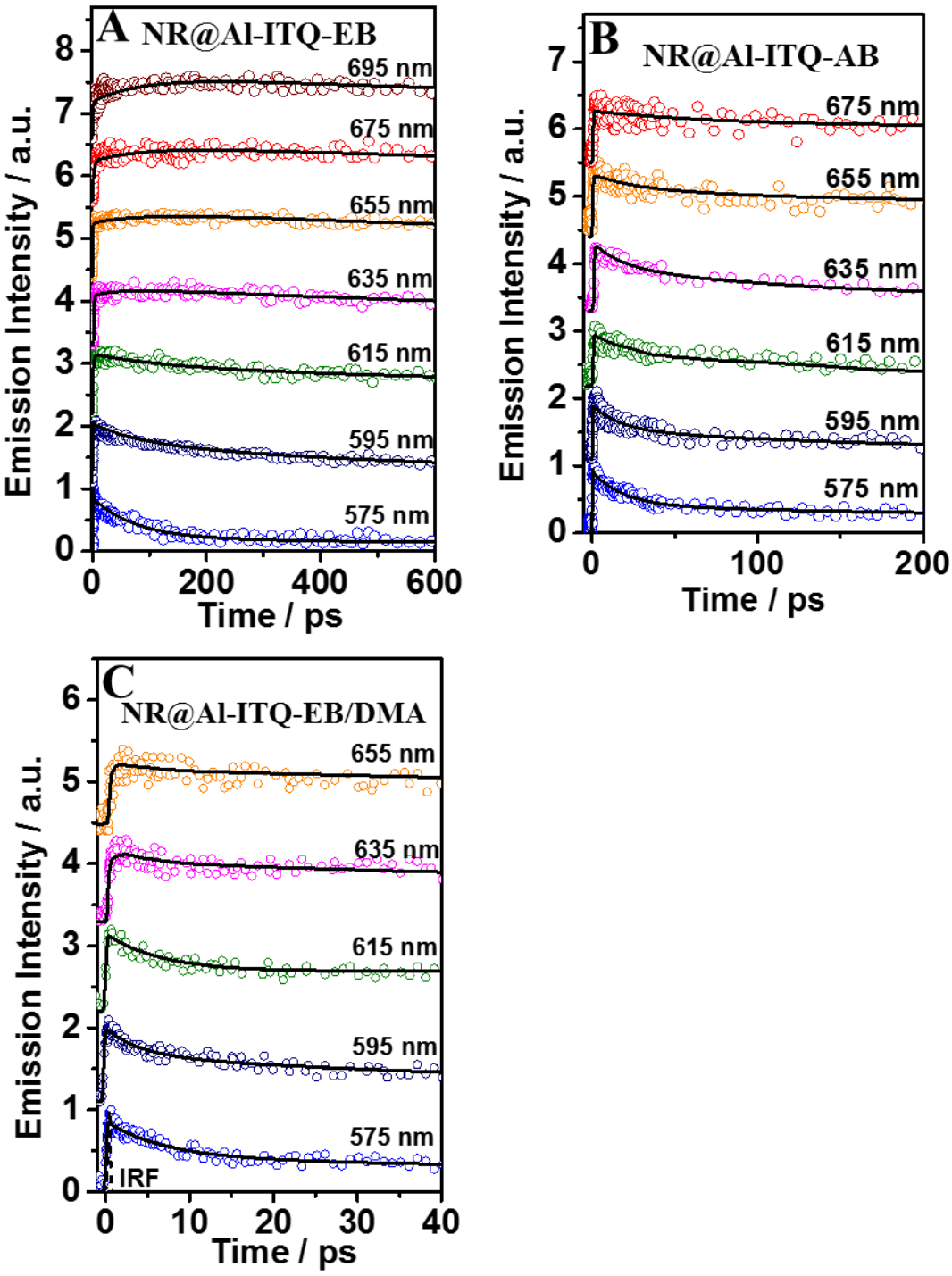
A NR@Al-ITQ-EB
695 nm
675 nm
655 nm
635 nm
615 nm
595 nm
575 nm
Emission Intensity / a.u.
Time / ps
B NR@Al-ITQ-AB
675 nm
655 nm
635 nm
615 nm
595 nm
575 nm
Emission Intensity / a.u.
Time / ps
C NR@Al-ITQ-EB/DMA
655 nm
635 nm
615 nm
595 nm
575 nm
IRF
Emission Intensity / a.u.
Time / ps

Figure 4:

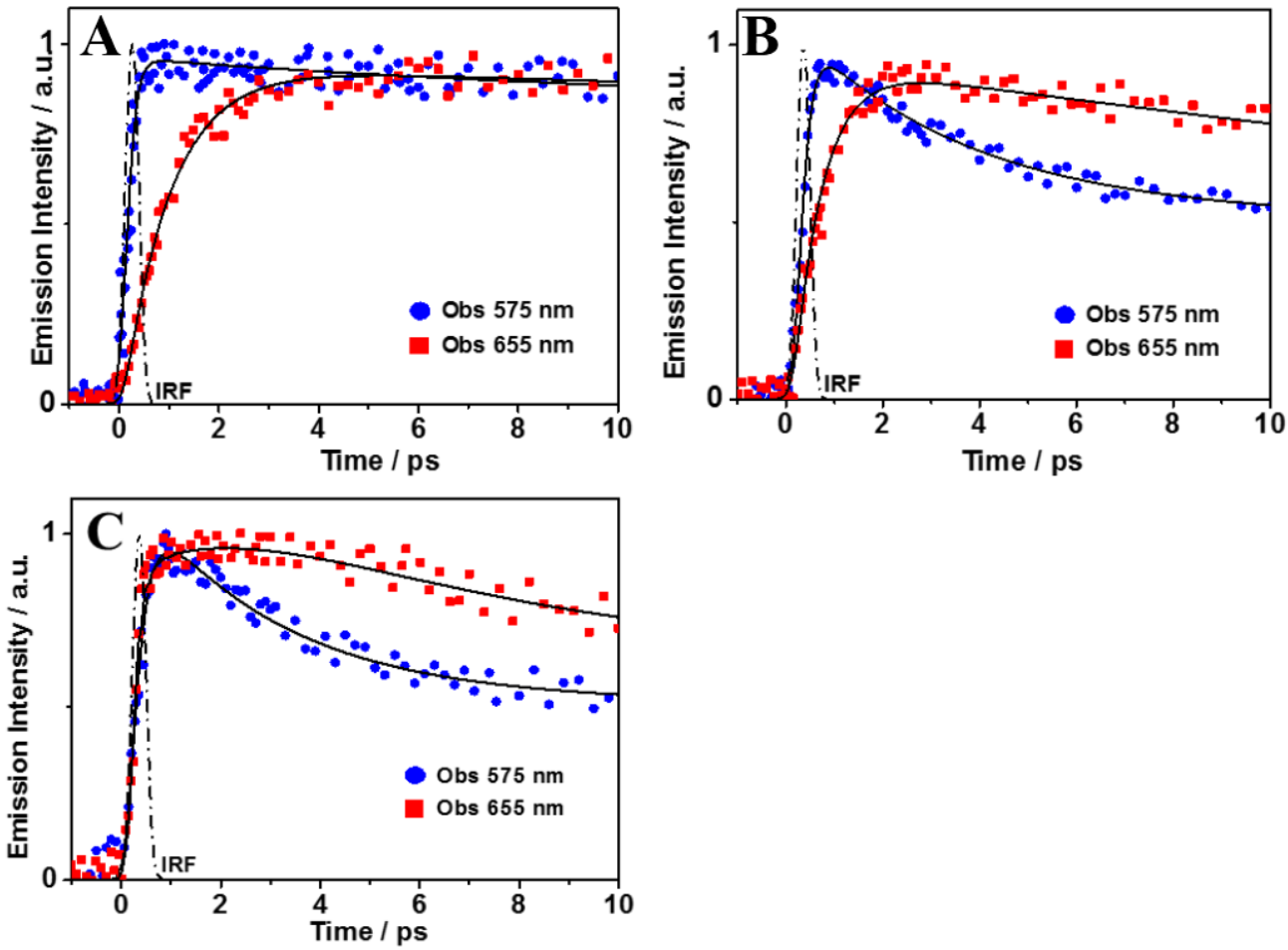
A
B
C
Emission Intensity / a.u.
Time / ps
Obs 575 nm
Obs 655 nm
IRF
0
1
0
2
4
6
8
10

Scheme 1:

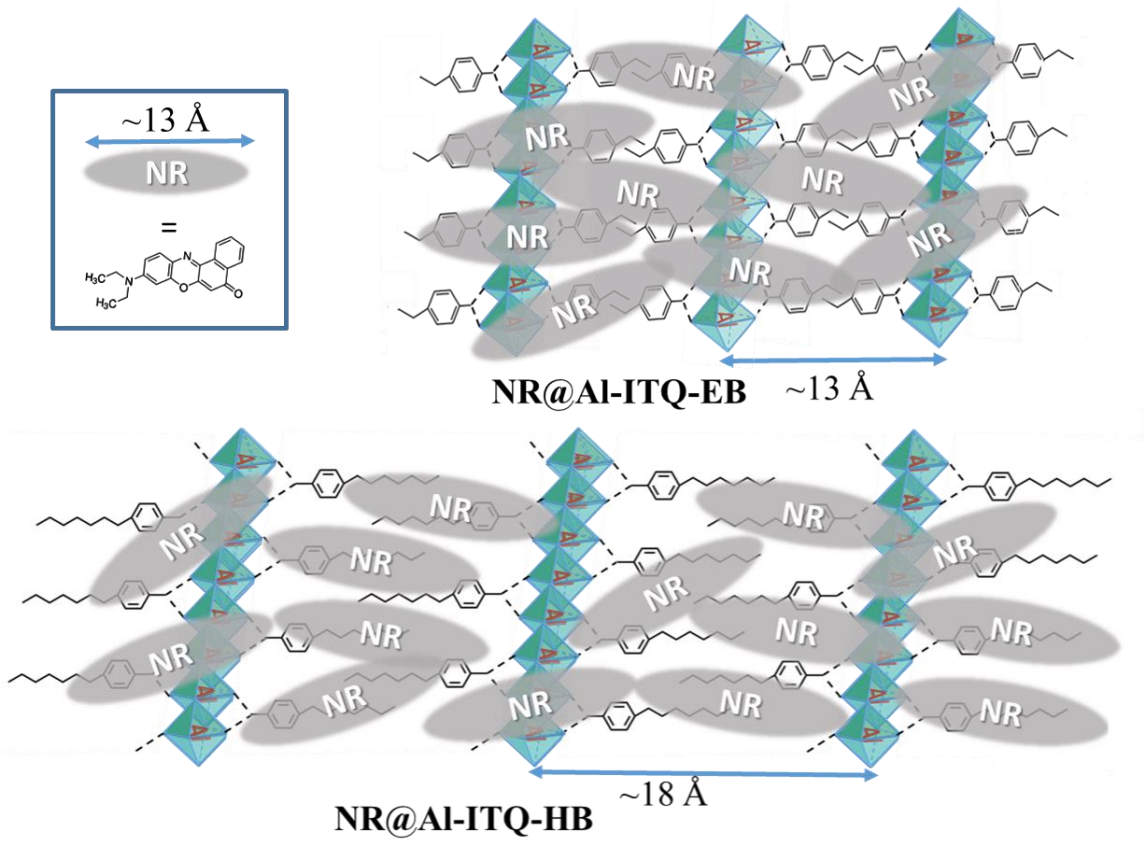

Scheme 2:

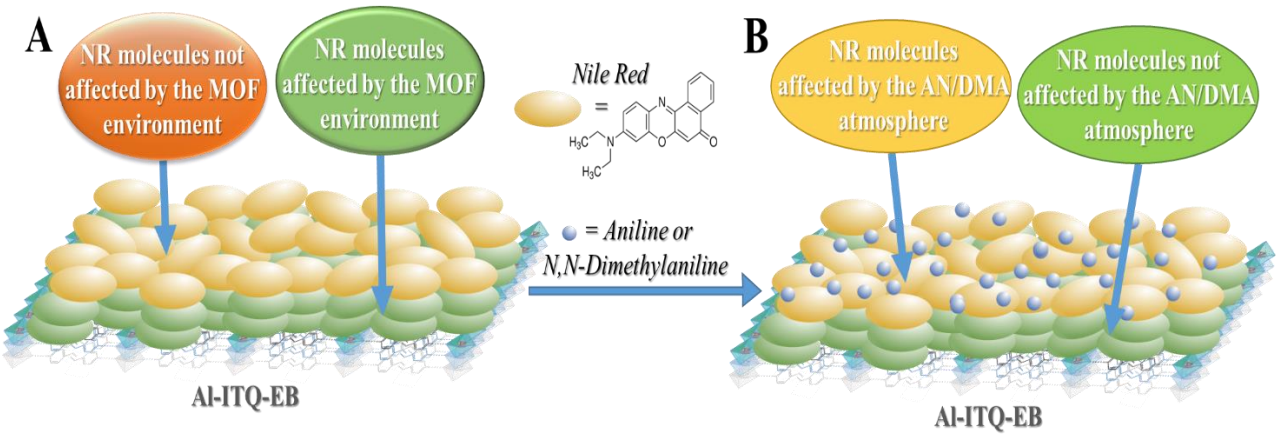

Scheme 3:

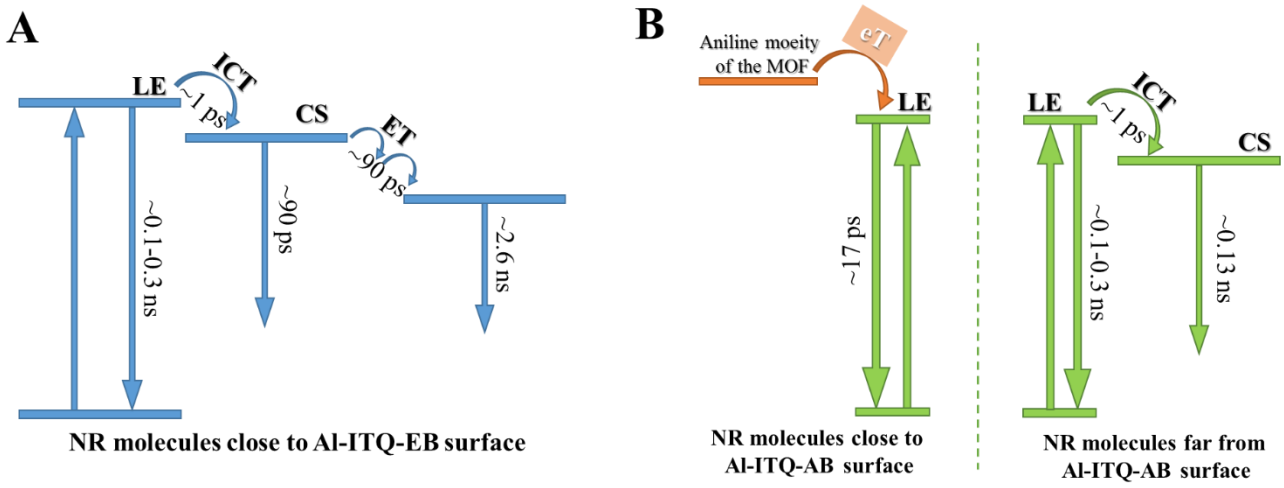

Table 1:

Sample	$\lambda_{Obs/nm}$	τ_1/ns (±0.05)	a_1	c_1	τ_2/ns (±0.15)	a_2	c_2	τ_3/ns (±0.40)	a_3	c_3
NR@Al-ITQ-EB	575	0.09	78	30	0.93	19	48	2.59	3	22
	600		43	8		44	51		13	41
	650		-100	-100		37	17		63	83
	700		-100	-100		33	15		67	85
	750		-100	-100		25	11		75	89
	775		-100	-100		24	10		76	90
NR@Al-ITQ-AB	575	0.13	67	22	0.54	24	33	2.10	9	45
	600		71	29		24	41		5	30
	650		60	21		33	46		7	33
	700		63	22		31	46		6	32
	750		66	25		29	46		5	29
	775		70	29		26	45		4	26
NR@Al-ITQ-EB / DMA	575	0.15	81	45	0.71	18	49	2.25	1	6
	600		63	22		33	57		4	21
	650		44	9		36	34		20	57
	700		40	7		38	33		22	60
	725		39	6		37	32		24	62
	750		39	6		38	33		23	61

Table 2.

$\lambda_{Obs/nm}$	τ_1/ps (±0.2)	a_1	τ_2/ps (±15)	a_2	τ_3/ns	a_3
575	1.3	7	91	76		17
595	1.2	9	86	32		59
615	1.4	-100	-	-		100
635	1.2	-84	85	-16	2.59*	100
655	1.0	-60	93	-40		100
675	1.4	-51	87	-49		100
695	1.3	-41	90	-59		100

*Fixed values in the fit.

Table 3:

$\lambda_{Obs/nm}$	τ_1/ps (±0.2)	a_1	τ_2/ps (±2)	a_2	τ_3/ps (±15)	a_3	τ_4/ps	a_4
575	1.0	10	16	44		-		46
595	1.1	3	17	56		-		41
615	1.0	3	16	40	115	25		32
635	-	-	18	39	114	30	540*	31
655	0.9	-100	19	25	116	4		71
675	1.0	-100	17	5	115	1		94

*Fixed values in the fit.

Table 4:

$\lambda_{Obs/nm}$	τ_1/ps (±0.2)	a_1	τ_2/ps (±2)	a_2	τ_3/ns	a_3
575	1.4	8	15	58		34
595	1.5	8	15	33		55
615	-	-	17	37	2.25*	54
635	1.4	-100	17	38		62
655	1.4	-100	17	38		62

*Fixed values in the fit.

Table 5.

Process	**NR@Al-ITQ-HB***	**NR@Al-ITQ-EB**	**NR@Al-ITQ-AB**	**NR@Al-ITQ-EB/DMA**	**NR/AN**
ET / ps	220	87	-	-	-
eT / ps	-	-	17	17	17
ICT / ps	0.5	1.2	1.0	1.4	1.0

* From ref. 23

Table of Contents